

Original Article

The effect of β -caryophyllene on nonalcoholic steatohepatitis

Naoya Arizuka¹, Tomoaki Murakami¹, and Kazuhiko Suzuki^{1*}

¹Laboratory of Veterinary Toxicology, Cooperative Department of Veterinary Medicine, Tokyo University of Agriculture and Technology, 3-5-8 Saiwai-cho, Fuchu, Tokyo 183-8509, Japan

Abstract: The pathogenesis of nonalcoholic steatohepatitis (NASH) is not fully understood, but many studies have suggested that oxidative stress plays a key role. The methionine- and choline-deficient diet (MCD) administration model can reproduce histopathological features of human NASH and is widely used for investigating NASH. C57BL/6J mice have been used in many studies, but strain differences in pathogenesis have not been sufficiently investigated. We administered MCD to two mouse strains and then compared difference between strains and investigated the effects of β -caryophyllene (BCP), which possesses an antioxidant effect, on development and progression of NASH. ICR and C57BL/6J mice were administered a control diet, MCD, MCD containing 0.02% BCP, or MCD containing 0.2% BCP. After 4 or 8 weeks, mice were sacrificed. In both strains, MCD administration induced hepatic steatosis and inflammation. These lesions were more severe in C57BL/6J mice than ICR mice, and liver fibrosis was observed at 8 weeks in C57BL/6J mice. These changes were attenuated by BCP coadministration. The mRNA expression of monocyte chemoattractant and activating factor (MCP)-1 and fibrosis-related factors increased in C57BL/6J mice, and these increases were reduced by BCP coadministration. The mRNA expression of antioxidant-related factors decreased in both strains, and these decreases were attenuated by BCP coadministration. Based on these results, the C57BL/6J mouse was a more suitable model for MCD-induced NASH than the ICR mouse. In addition, it was suggested that antioxidant effect of BCP might suppressed the damage of hepatocytes caused by oxidative stress and following inflammation and fibrosis. (DOI: 10.1293/tox.2017-0018; J Toxicol Pathol 2017; 30: 263–273)

Key words: antioxidant, β -caryophyllene, methionine- and choline-deficient diet, nonalcoholic steatohepatitis, oxidative stress

Introduction

Nonalcoholic fatty liver disease (NAFLD) is a relatively prevalent liver disease that is recognized as an important health concern^{1,2}, and it is estimated that one billion people have NAFLD worldwide now³. NAFLD is characterized by the accumulation of hepatic lipid⁴, and the majority of patients have a benign prognosis, i.e., nonalcoholic fatty liver (NAFL), but up to 25% of patients develop potentially progressive liver damage, i.e., nonalcoholic steatohepatitis (NASH). A growing body of literature shows the close relationship of steatohepatitis with metabolic syndrome, which is characterized by abdominal obesity, insulin resistance with or without frank hyperglycemia, dyslipidemia, and hypertension, and several recent studies have documented the association of NASH with metabolic syndrome^{5–8}. However, this association is not universal, and the pathogenesis of NASH, especially the mechanism by which NAFL pro-

gresses to NASH, remains poorly understood^{9–11}.

A large number of studies regarding the pathophysiology and treatment of NASH have been undertaken in mouse models of human NASH, such as dietary models including a methionine- and choline-deficient diet (MCD), choline-deficient L-amino-acid defined diet, and high-fat diet, and genetic models, such as ob/ob mice, db/db mice, KK-Ay/a mice, and phosphatase and tensin homolog null mice. However, all of the animal models have had their own merits and demerits, and none have been able to fully reproduce the pathogenic mechanisms and histological features observed in humans. Among the models, the MCD administration model is able to reproduce most of the histopathological features of human NASH^{12,13} and reproduce NASH within a relatively shorter feeding time than other dietary models of NASH. In addition, a previous study reported that MCD administration activated mechanisms that have been implicated in human NASH progression; thus, this diet model is ideal for studying mechanisms driving NASH-related inflammation/fibrosis, as well as strategies to inhibit these processes¹⁴. C57BL/6J mice have been widely used for MCD-induced NASH models in many studies, but strain differences in sensitivity to MCD have not been sufficiently investigated. Therefore, comparing the differences between strains may lead to determination of a strain that is more suitable for use as a NASH model induced by MCD administration.

Histologically, NASH is similar to alcohol-induced liv-

Received: 1 March 2017, Accepted: 29 May 2017

Published online in J-STAGE: 19 June 2017

*Corresponding author: K Suzuki (e-mail: kzsuzuki@cc.tuat.ac.jp)

©2017 The Japanese Society of Toxicologic Pathology

This is an open-access article distributed under the terms of the Creative Commons Attribution Non-Commercial No Derivatives

(by-nc-nd) License. (CC-BY-NC-ND 4.0: <https://creativecommons.org/licenses/by-nc-nd/4.0/>).



er disease, suggesting that it might have some similar features with respect to pathogenesis. Among the multiple factors involved in the process of alcohol-induced liver injury, a crucial role is played by oxidative stress¹⁵. In addition, a previous study reported that free radicals from NADPH oxidase in hepatic Kupffer cells play a predominant role in the pathogenesis of early alcohol-induced hepatitis¹⁶. Similarly, many studies suggested that hepatic oxidative stress plays a key role in the pathogenesis of NASH, and the failure of antioxidant defense mechanisms against oxidative stress is an important factor in the pathogenesis of NASH^{8, 17–19}. Thus, it was estimated that antioxidant supplementations might suppress development and progression of NASH, and its effect was investigated in some studies^{9, 20, 21}. However, fundamental medications for NASH have not been established.

β -caryophyllene (BCP) is a sesquiterpene found in various plants including clove, cinnamon leaves, and copaiba balsam. BCP is known to possess anti-inflammatory^{22, 23}, anticarcinogenic²⁴, antibiotic^{23, 25}, and local anaesthetic²⁶ activities. In addition to these effects, BCP also has an antioxidant effect^{23, 27}. A previous study reported that BCP protected rat livers from carbon tetrachloride toxicity via its antioxidant activity²⁸. In this study, we investigated i) the strain differences in MCD-induced liver lesions by using ICR and C57BL/6J mice and ii) the effect of BCP on MCD-induced progression of NAFL to NASH.

Materials and Methods

Chemicals

BCP was purchased from SigmaA-Aldric (Tokyo, Japan). All other chemicals were obtained commercially.

Experimental design

Forty male ICR mice, 5 weeks old, and forty male C57BL/6J mice, 5 weeks old, were purchased from Charles River Laboratories Japan (Kanagawa, Japan) and SLC Japan (Shizuoka, Japan), respectively. Mice were housed in a temperature-controlled room with 12-h-light/12-h-dark cycling and allowed free access to tap water and control diet (CD, Oriental Yeast Co., Ltd., Tokyo, Japan).

In each strain, mice were acclimatized for 1 week and divided into four groups administrated a control diet (CD), MCD (MCD), MCD containing 0.02% BCP (MCD + L), and MCD containing 0.2% BCP (MCD + H). These doses were determined with reference to the results of examination by others²⁹. During the experimental period, body weight was measured once per week. At the end of the respective experiment, which lasted 4 or 8 weeks, 5 mice per group were sacrificed by exsanguination from the abdominal aorta under isoflurane anesthesia. Livers were excised and weighed. For histopathology and immunohistochemistry, the liver obtained from each mouse was fixed by the PLP (periodate-lysine-paraformaldehyde)-AMeX (acetone, methyl benzoate, and xylene)³⁰. In brief, specimens were immersed in PLP fixative (containing 4% paraformaldehyde) for 7 hours at 4°C and then washed with phosphate-buffered saline (PBS;

0.01 M, pH 7.4) for 2 hours at 4°C. Then, the tissues were dehydrated in acetone overnight at 4°C and for 1 hour twice at room temperature, cleared in methyl benzoate for 30 minutes twice and in xylene for 30 minutes twice, soaked in paraffin for 40 minutes three times at 60°C, and embedded in paraffin. The paraffin blocks prepared by the PLP-AMeX method were kept at 4°C. The liver tissues for PCR were collected by cutting them into small pieces, frozen, and then preserved at -80°C.

Blood biochemistry

Alanine aminotransferase (ALT) and triglyceride (TG) were measured in serum samples from each mouse at 8 weeks.

Histopathology

Two-micrometer sections were stained with hematoxylin and eosin (HE) and Sirius Red. Histological scores were measured with NAFLD activity score (NAS) recommended by the Pathology Committee of the NASH Clinical Research Network³¹. The minimum histological criterion for the diagnosis of NASH was the presence of steatosis associated with hepatocellular ballooning involving zone 3 and lobular inflammatory infiltration³². Therefore, in NAS, these findings were semiquantitatively scored as steatosis (score of 0–3), lobular inflammation (score of 0–3), and hepatocellular ballooning (score of 0–2), then, the unweighted sum of these scores was obtained as activity score (0–8). An activity score ≥ 5 was considered to indicate NASH, a score of 3 or 4 was considered to indicate borderline NASH, and a score of 0 to 2 was considered to indicate NAFL.

Immunohistochemistry

For immunohistochemistry, 2- μ m sections were deparaffinized and soaked in methanol containing 0.3% hydrogen peroxide for 30 minutes to block endogenous peroxidase activity. Then, the sections were treated with 10% normal goat serum for 30 minutes to block nonspecific reaction. Anti-CD3 antibody (rabbit polyclonal, Abcam plc, Cambridge, UK) and anti-F4/80 antibody (rat monoclonal, Bio-Rad Laboratories Inc., Hercules, CA, USA) were applied as the primary antibodies overnight at 4°C. In the case of CD3, the sections were incubated with EnVision solution (Dako, Glostrup, Denmark) against rabbit immunoglobulin (Ig) G for 30 minutes at room temperature. In the case of F4/80, each section was incubated with anti-rat IgG (rabbit, Vector Laboratories Inc., Burlingame, CA, USA) for 30 minutes and then with a Vectastain ABC Kit (Vector Laboratories Inc., Burlingame, CA, USA) for 30 minutes. Antibody binding was visualized with 3,3'-diaminobenzidine chromogen and counterstaining with Mayer's hematoxylin. Tris-buffered saline (0.15 M NaCl, 0.05 M Tris-HCl, pH 7.6) was used for rinsing. With regard to CD3 and F4/80, the number of positive cells was counted in fifty fields per section at 200-fold magnification, and the average number per field was calculated.

Table 1. Sequences of the Primers Used for Real-time PCR

Target	Forward	Reverse
Inflammatory cytokine		
<i>Il1b</i>	GCAACTGTTCTGAACTCAACT	ATCTTTTGGGGTCCGTCAACT
<i>Il6</i>	TAGTCCTTCTACCCCAATTCC	TTGGTCCTTAGCCACTCCTTC
<i>Mcp1</i>	TTAAAAACCTGGATCGGAACCA	GCATTAGCTTCAGATTACGGG
Antioxidant related factors		
<i>Sod1</i>	GGTGAACCAGTTGTGTTGTC	CCGTCCTTCCAGCAGTC
<i>Sod2</i>	GACCTGCCTTACGACTATG	GAAGAGCGACCTGAGTTG
<i>Cat</i>	CAGGTGCGGACATTCTAC	TTGCGTTCTTAGGCTTCTC
<i>Gsr</i>	GGATTGGCTGTGATGAGATG	CTGAAGAGGTAGGATGAATGG
<i>Gpx1</i>	CAATCAGTTCGGACACCAGGAG	TCTCACCATTCACTTCGCACTTC
Fibrosis-related factors		
<i>Nox2</i>	GACCATTGCAAGTGAACACCC	AAATGAAGTGGACTCCACGCG
<i>Tgfb</i>	CACCATCCATGACATGAACC	TGGTTGTAGAGGGCAAGGAC
<i>Collagen1a1</i>	CCTCAGGGTATTGCTGGACAA	ACCACTTGATCCAGAAGGACCTT
House keeping gene		
β -actin	CCCTGGCTCCTAGCACCAT	AGAGCCACCAATCCACACAGA

Real-time reverse transcription polymerase chain reaction (real-time RT-PCR) analysis

Total RNA was extracted from liver tissue of each mouse using an RNeasy Mini Kit (QIAGEN, Venlo, Netherlands). The concentrations of total RNA samples were measured using Gen5 2.0 (BioTek Instruments, Inc., Winooski, VT, USA). Then, cDNA was prepared from 500 ng of total RNA using PrimeScript RT Master Mix (Takara Bio Inc., Kusatsu, Japan) in a Life ECO Thermal Cycler (Bioer Technology Co., Ltd, Hangzhou, China) (37°C for 15 minutes and 85°C for 5 seconds). Real-time PCR was performed using SYBR Premix Ex Taq II (Takara Bio Inc., Kusatsu, Japan) in a Thermal Cycler Dice Real Time System II (Takara Bio Inc., Kusatsu, Japan) (95°C for 30 seconds, 40 cycle of 95°C for 5 seconds and 60°C for 30 seconds, 95°C for 15 seconds, 60°C for 30 seconds, and 95°C for 15 seconds). Five targets for antioxidant-related factors (glutathione peroxidase (GPx1), glutathione reductase (GSR), catalase (CAT), superoxide dismutase (SOD) 1, and SOD2), and three targets for inflammatory cytokine (interleukin (IL)-1 β , IL-6, and monocyte chemotactic and activating factor (MCP)-1) and fibrosis-related factors (NADPH oxidase (Nox) 2, transforming growth factor (TGF)- β and Collagen I α 1) were analyzed. The primer sequences used were as listed in Table 1. The relative value of gene expression was calculated using standard curve values that were normalized to those of the β -actin gene, the endogenous control in the same sample, and then relative to a control value were obtained.

Statistical analysis

Obtained data were expressed as means and standard deviations. Statistical differences between groups were evaluated using the following methods: initially, numerical data were analyzed for homogeneity of variance using

Bartlett's test. Dunnett's test or Steel's test was then used when the variance was homogenous or heterogeneous among the groups, respectively. A difference was considered to be significant at $P < 0.05$.

Results

Body weight and liver weight

In both strains, suppressed body weight gain was observed in MCD-fed groups, and this was ameliorated by a higher dose of BCP coadministration at 8 weeks. In ICR mice, the relative liver weight was not different among the groups at 4 weeks, but it was decreased by MCD administration and attenuated by a higher dose of BCP coadministration at 8 weeks. In the C57BL/6J mice, the relative liver weight was decreased by MCD administration at both 4 and 8 weeks, and an attenuating effect was observed in the MCD + H group at 8 weeks (Table 2).

Blood biochemistry

In ICR mice, ALT and TG were not significantly different among the groups. In C57BL/6J mice, ALT was significantly increased by MCD administration, and this increase was significantly reduced by BCP coadministration. Moreover, TG was significantly decreased by MCD administration, but this decrease was not attenuated by BCP coadministration (Table 3).

Histopathology

CD administration did not induce any histological changes (Fig. 1A, 1B). In ICR mice, MCD administration induced mild steatosis, some inflammatory foci consisting mainly mononuclear cells, and a small amount of ballooning degeneration of hepatocytes at 4 weeks, and these findings

Table 2. Body and Liver Weights

		4 wk				8 wk				
		CD	MCD	MCD+L	MCD+H	CD	MCD	MCD+L	MCD+H	
Final Body weight (g)	ICR	30.59 \pm 3.59	18.76 \pm 2.09*	20.89 \pm 1.83*	18.78 \pm 1.30*	37.99 \pm 6.08	16.92 \pm 0.95 [£]	18.70 \pm 1.54 [£]	25.79 \pm 1.42 ^{£‡}	
	C57BL	24.74 \pm 0.69	15.42 \pm 0.92*	14.86 \pm 0.36*	15.38 \pm 0.45*	28.83 \pm 1.58	14.01 \pm 0.96*	13.60 \pm 0.73*	16.04 \pm 1.11* [†]	
Liver weight	Absolute (g)	ICR	1.40 \pm 0.36	0.66 \pm 0.12 [£]	0.81 \pm 0.09	0.71 \pm 0.04 [£]	1.81 \pm 0.24	0.63 \pm 0.05 [£]	0.75 \pm 0.12 [£]	1.10 \pm 0.12 ^{£‡}
		C57BL	1.06 \pm 0.05	0.49 \pm 0.01 [£]	0.48 \pm 0.05 [£]	0.46 \pm 0.02 [£]	1.64 \pm 0.11	0.44 \pm 0.04 [£]	0.40 \pm 0.03 [£]	0.58 \pm 0.12 [£]
	Relative (g/100 g BW)	ICR	4.52 \pm 0.82	3.49 \pm 0.39	3.87 \pm 0.14	3.80 \pm 0.29	4.79 \pm 0.34	3.70 \pm 0.23*	4.01 \pm 0.47*	4.25 \pm 0.29 [†]
		C57BL	4.30 \pm 0.14	3.17 \pm 0.14*	3.20 \pm 0.30*	3.02 \pm 0.20*	5.17 \pm 0.18	3.16 \pm 0.21 [£]	2.94 \pm 0.20 [£]	3.90 \pm 0.14 [£]

Data are represented as the mean \pm SD. * P <0.05 compared with each CD group (Dunnett's test). [†] P <0.05 compared with each MCD group (Dunnett's test). [£] P <0.05 compared with each CD group (Steel-Dwass test). [‡] P <0.05 compared with each MCD group (Steel-Dwass test).

Table 3. Blood Biochemistry at 8 Weeks

		CD	MCD	MCD+L	MCD+H
		ALT	ICR	16.25 \pm 5.50	10.40 \pm 4.87
	C57BL	13.50 \pm 11.32	67.75 \pm 25.95*	49.67 \pm 11.59*	23.25 \pm 14.43 [†]
TG	ICR	65.00 \pm 13.85	67.25 \pm 25.03	55.25 \pm 17.21	55.60 \pm 20.51
	C57BL	108.50 \pm 16.01	21.00 \pm 2.64*	19.00 \pm 4.35*	32.40 \pm 8.50*

Data are represented as the average \pm SD. * P <0.05 compared with each CD group (Dunnett's test). [†] P <0.05 compared with each MCD group (Dunnett's test).

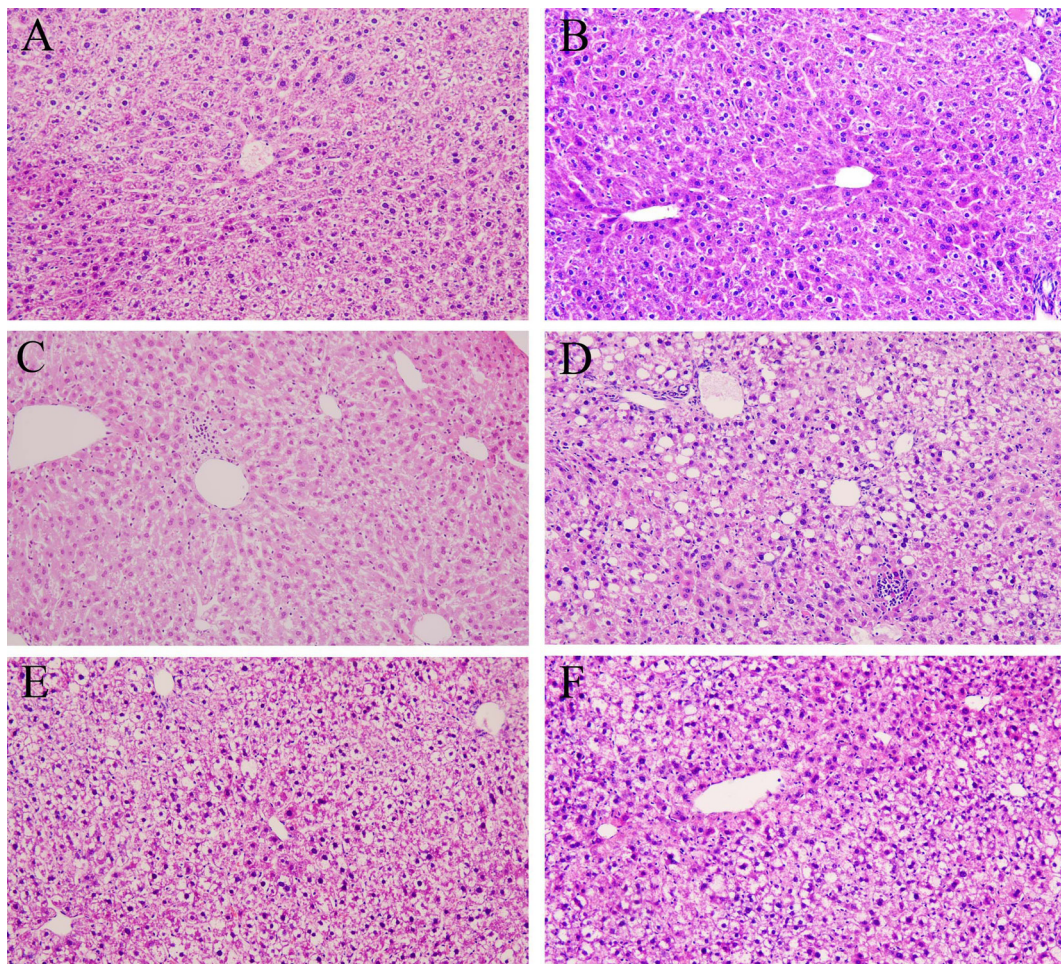


Fig. 1. Histopathology in ICR (A, C, E) and C57BL/6J (B, D, F) mice. Mice were administered the control diet (A, B), MCD (C, D), or MCD containing 0.2% BCP (E, F) for 8 weeks. HE stain, $\times 200$.

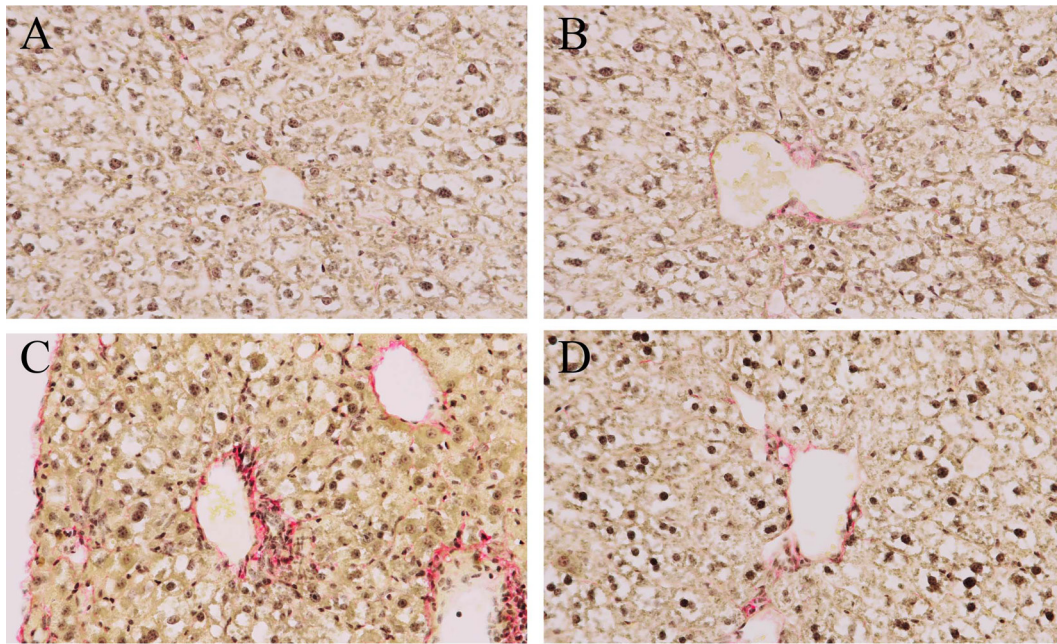


Fig. 2. Liver fibrosis during experimental steatohepatitis in ICR (A, B) and C57BL/6J (C, D) mice. Mice were administered the control diet (A), MCD (B, C), or MCD containing 0.2% BCP (D) for 8 weeks. Sirius Red stain, $\times 400$

Table 4. Histological Scores by NAS

		4wk				8wk			
		CD	MCD	MCD+L	MCD+H	CD	MCD	MCD+L	MCD+H
Steatosis	ICR	0.00 \pm 0.00	1.20 \pm 0.44 [£]	0.60 \pm 0.54	0.60 \pm 0.54	0.00 \pm 0.00	1.60 \pm 0.54 [£]	1.20 \pm 0.44 [£]	1.00 \pm 0.00 ^{£‡}
	C57BL	0.00 \pm 0.00	1.80 \pm 0.44 [£]	2.00 \pm 0.00 [£]	1.80 \pm 0.50 [£]	0.00 \pm 0.00	2.00 \pm 0.00 [£]	1.60 \pm 0.54 [£]	1.00 \pm 0.70
Inflammation	ICR	0.00 \pm 0.00	1.20 \pm 0.44 [£]	0.80 \pm 0.44	0.80 \pm 0.44	0.00 \pm 0.00	1.00 \pm 0.00 [£]	0.80 \pm 0.44	0.40 \pm 0.54
	C57BL	0.20 \pm 0.44	1.00 \pm 0.00	0.80 \pm 0.83	1.00 \pm 0.00	0.60 \pm 0.54	1.60 \pm 0.54	1.00 \pm 0.00	1.20 \pm 0.44
Ballooning	ICR	0.00 \pm 0.00	0.40 \pm 0.54	0.00 \pm 0.00	0.00 \pm 0.00	0.00 \pm 0.00	1.20 \pm 0.44 [£]	1.00 \pm 0.00 [£]	0.40 \pm 0.54
	C57BL	0.00 \pm 0.00	1.20 \pm 0.44 [£]	0.80 \pm 0.44	0.30 \pm 0.50	0.00 \pm 0.00	1.00 \pm 0.00 [£]	0.60 \pm 0.54	0.20 \pm 0.44
Activity score	ICR	0.00 \pm 0.00	2.80 \pm 1.30 [£]	1.40 \pm 0.54 [£]	1.40 \pm 0.54 [£]	0.00 \pm 0.00	3.80 \pm 0.80 [£]	3.00 \pm 0.70 [£]	1.80 \pm 1.00 [£]
	C57BL	0.20 \pm 0.44	4.00 \pm 0.70 [£]	3.60 \pm 1.14 [£]	3.00 \pm 0.00 [£]	0.60 \pm 0.54	4.60 \pm 0.54 ^{*£}	3.20 \pm 0.83 ^{*†}	2.40 \pm 1.14 ^{*†}

Range of the respective scores: steatosis, 0–3; inflammation, 0–3; ballooning, 0–2; activity score, 0–8. Data are represented as mean \pm S.D. * P <0.05 compared with each CD group (Dunnett's test). † P <0.05 compared with each MCD group (Dunnett's test). £ P <0.05 compared with each CD group (Steel-Dwass test). ‡ P <0.05 compared with each MCD group (Steel-Dwass test).

were slightly worse at 8 weeks (Fig. 1C). Their severities were slightly reduced by BCP coadministration (Fig. 1E). In C57BL/6J mice, more pronounced lesions were observed and were more severe at 8 weeks (Fig. 1D) than 4 weeks. The severities of these lesions were reduced by BCP coadministration (Fig. 1F). Distinct Fibrosis was not observed in any groups in ICR mice at 4 and 8 weeks (Fig. 2A, 2B), but it was observed primarily in the pericentral areas in C57BL/6J mice at 8 weeks (Fig. 2C). It was also mildly inhibited by BCP coadministration (Fig. 2D). When the severity of lesions was scored using the NAS (Table 4), the activity scores of the ICR and C57BL/6J mice in the MCD groups were 2.8 ± 1.3 and 4.0 ± 0.7 at 4 weeks. These scores were mildly reduced by high dose of BCP coadministration in both strains (1.4 ± 0.5 in the ICR mice and 3.0 ± 0.0 in the

C57BL/6J mice). At 8 weeks, the activity scores of the ICR and C57BL/6J mice in the MCD groups were 3.8 ± 0.8 and 4.6 ± 0.5 , and the scores were significantly reduced by a high dose of BCP coadministration in C57BL/6J mice (1.8 ± 1.0 in the ICR mice and 2.4 ± 1.1 in the C57BL/6J mice).

Changes in infiltrated mononuclear cells

In ICR mice, the number of CD3-positive cells was moderately increased by MCD administration and was mildly but not significantly decreased by BCP coadministration at both 4 and 8 weeks (Fig. 3A, 3B, 3D, 3F). The number of F4/80-positive cells was not significantly different among the groups at both 4 and 8 weeks (Fig. 4A, 4B, 4F). In C57BL/6J mice, the numbers of CD3- and F4/80-positive cells were moderately increased by MCD administration,

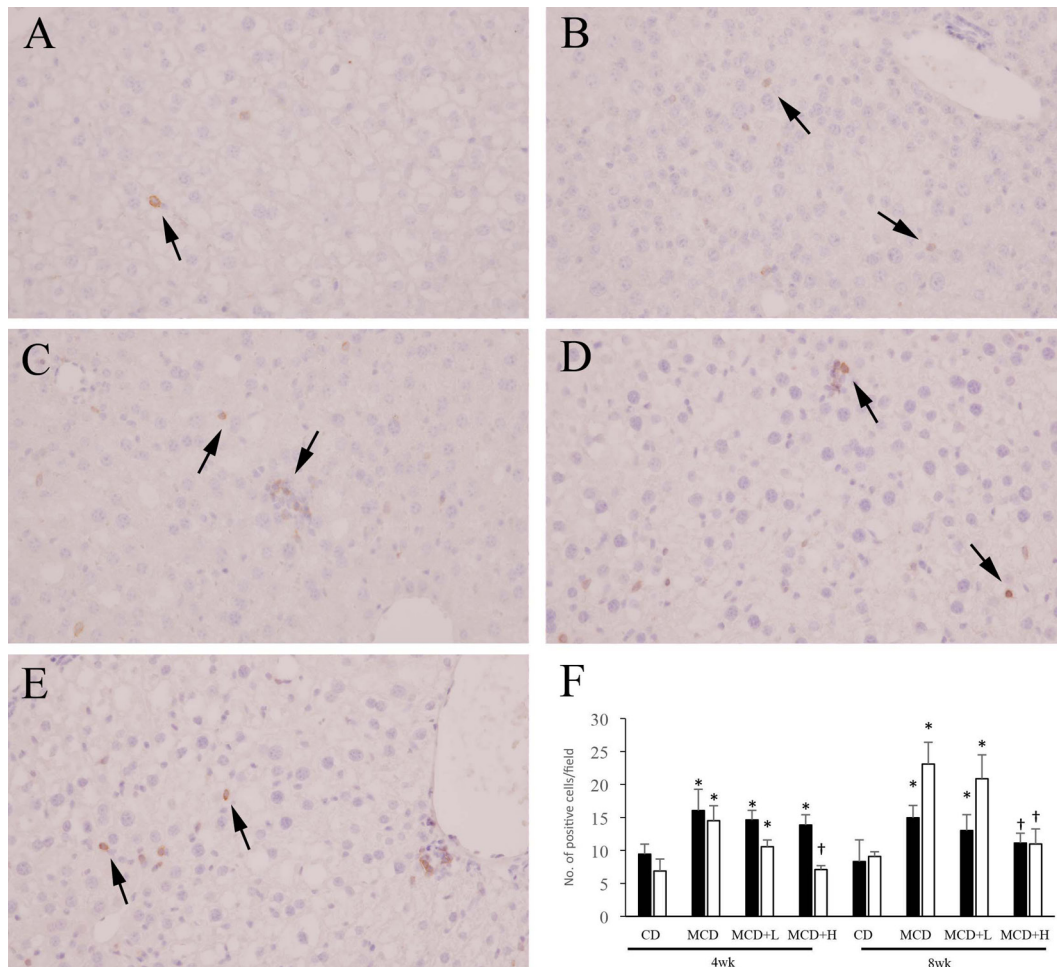


Fig. 3. Immunohistochemistry for CD3 in ICR (A, B, D) and C57BL/6J (C, E) mice. Mice were administered the control diet (A), MCD (B, C), or MCD containing 0.2% BCP (D, E) for 8 weeks. $\times 400$. Arrows indicate positive cells. The number of positive cells (F). ■, ICR mouse; □, C57BL/6J mouse. Data are represented as the mean \pm SD. * $P < 0.05$ compared with each CD group (Dunnett's test). † $P < 0.05$ compared with each MCD group (Dunnett's test).

and these increases were ameliorated by BCP coadministration at both 4 and 8 weeks (Fig. 3C, 3E, 3F, 4C–4F).

Changes in mRNA expression

Changes in the mRNA expression of genes in the liver are shown in Table 5. In ICR mice, the mRNA expression levels of IL-1 β and IL-6 increased in the MCD group, and these increases were reduced by BCP coadministration at 8 weeks. On the other hand, the mRNA expression of MCP-1 showed no significant difference between the groups at both 4 and 8 weeks. In contrast, in C57BL/6J mice, the mRNA expression levels of IL-1 β and IL-6 showed no significant difference between the groups at both 4 and 8 weeks. On the other hand, the mRNA expression of MCP-1 showed a tendency to increase as a result of MCD administration for 8 weeks, and this increase was reduced by BCP coadministration.

Regarding the antioxidant-related factors, the mRNA expression levels of SOD1, SOD2, and GPx1 were decreased by MCD administration, and these decreases were re-

duced by BCP coadministration in ICR mice at 8 weeks. In C57BL/6J mice, in addition to SOD1, SOD2 and GPx1, another antioxidant-related factor was also decreased by MCD administration, and the decreases in all four factors were reduced by BCP coadministration. The mRNA expression levels of fibrosis-related factors, Nox2, TGF- β , and Collagen I α 1, were not significantly different between the groups in ICR mice at both 4 and 8 weeks, but in C57BL/6J mice, these expression levels were increased by MCD administration and the increases were attenuated by BCP coadministration at 8 weeks.

Discussion

NASH is now recognized as an important health concern, and the incidence of NASH has been rising worldwide. Nevertheless, the pathogenesis of NASH is still not fully understood, and thus many rodent models have been proposed to investigate it. Among these models, the use of an essential amino acids-deficient diet, such as the MCD, is well accept-

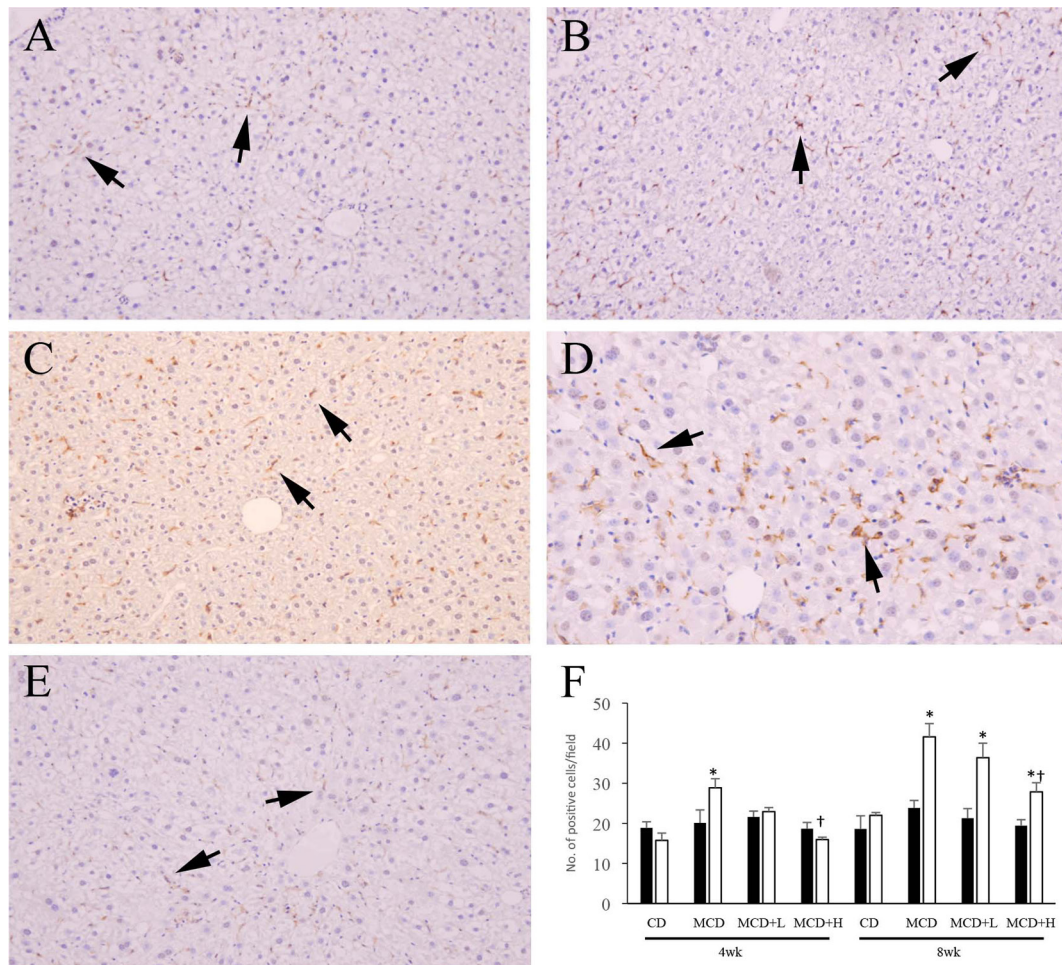


Fig. 4. Immunohistochemistry for F4/80 in ICR (A, B) and C57BL/6J (C, D, E) mice. Mice were administered the control diet (A), MCD (B, C, D), or MCD containing 0.2% BCP (E) for 8 weeks. A–C, E: $\times 200$. D: $\times 400$. Arrows indicate positive cells. The number of positive cells (F). ■, ICR mouse; □, C57BL/6J mouse. Data are represented as the mean \pm SD. * $P < 0.05$ compared with each CD group (Dunnett's test). † $P < 0.05$ compared with each MCD group (Dunnett's test).

ed because it reproduces many histopathological features of human cases, including fibrotic disorders associated with hepatic lipid accumulation and the presence of inflammation. When the MCD-induced mouse NASH model was produced, the C57BL/6J mouse was widely used³³. However, strain differences in the sensitivity to MCD have not been sufficiently investigated. Thus, we used ICR mice to compare strain differences in lesions produced by MCD administration. MCD administration induced hepatic steatosis and inflammation in both strains, and the hepatic steatosis and inflammation were more severe at 8 weeks than 4 weeks. However, the histological changes in ICR mice were milder than those in C57BL/6J mice. When the severity of lesions was scored using the NAS, some C57BL/6J mice received high activity scores (≥ 5), which was considered to indicate NASH, at 4 weeks. On the other hand, 4 out of 5 ICR mice were diagnosed by NAS as having borderline NASH even at 8 weeks. The average activity score in ICR mice at 8 weeks (3.80 ± 0.80) was slightly lower than that in C57BL/6J mice at 4 weeks (4.00 ± 0.70). As for blood biochemistry, an in-

creased ALT level was observed only in C57BL/6J mice (Table 3). Therefore, it was suggested that MCD administration for 4 weeks could induce NASH in C57BL/6J mice and that it progress earlier and is more severe than in ICR mice. Methionine and choline are essential components for very-low-density lipoprotein (VLDL) and lipid oxidation³⁴. A deficiency of these components can reduce lipid oxidation and lipid transport outside of hepatocyte, resulting in lipid accumulation in the liver. Thus, the strain difference observed in this study may be due to a difference in lipid metabolism.

Some NASH patients progress to liver fibrosis (cirrhosis), and this progression is a critical problem because cirrhosis can progress to hepatocellular carcinoma^{35, 36}. In our experiment, liver fibrosis was observed in C57BL/6J mice at 8 weeks as a result of MCD administration, but it was not seen in ICR mice. This result for C57BL/6J mice is consistent with the results of previous study³⁷. In addition, the number of F4/80-positive macrophages increased over time during the experimental period, but the increase was significant only in C57BL/6J mice. Macrophage-induced nuclear

Table 5. Change in the mRNA Expression

		4wk				8wk			
		CD	MCD	MCD+L	MCD+H	CD	MCD	MCD+L	MCD+H
Inflammatory cytokine									
<i>Il1b</i>	ICR	1.00 ± 0.43	1.59 ± 0.66	2.44 ± 1.20*	1.45 ± 0.56	1.00 ± 0.37	2.34 ± 0.77*	2.17 ± 0.75*	1.10 ± 0.53†
	C57BL	1.00 ± 0.46	1.06 ± 0.30	0.86 ± 0.37	0.96 ± 0.39	1.00 ± 0.40	0.71 ± 0.44	1.58 ± 0.02	0.99 ± 0.24
<i>Il6</i>	ICR	1.00 ± 0.67	3.42 ± 1.66	2.05 ± 0.75	1.26 ± 0.60	1.00 ± 0.51	2.87 ± 0.68*	1.73 ± 0.70†	0.71 ± 0.20†
	C57BL	1.00 ± 0.50	1.06 ± 0.50	1.65 ± 0.35	0.88 ± 0.26	1.00 ± 0.54	0.71 ± 0.43	0.96 ± 0.28	1.00 ± 0.74
<i>Mcp1</i>	ICR	1.00 ± 0.49	1.46 ± 0.16	1.36 ± 0.48	0.65 ± 0.39†	1.00 ± 0.87	1.06 ± 0.51	1.14 ± 0.44	0.71 ± 0.20
	C57BL	1.00 ± 0.54	2.19 ± 1.19	2.13 ± 1.36	2.50 ± 0.53	1.00 ± 0.24	15.19 ± 4.13	6.62 ± 2.16	6.63 ± 5.39
Antioxidant related factors									
<i>Sod1</i>	ICR	1.00 ± 0.45	0.63 ± 0.26	0.55 ± 0.15	0.66 ± 0.41	1.00 ± 0.24	0.69 ± 0.03	0.72 ± 0.08‡	0.98 ± 0.09‡
	C57BL	1.00 ± 0.18	0.37 ± 0.10*	0.49 ± 0.13*	0.49 ± 0.06*	1.00 ± 0.20	0.56 ± 0.03*	0.71 ± 0.09	0.82 ± 0.22
<i>Sod2</i>	ICR	1.00 ± 0.17	0.72 ± 0.21	0.83 ± 0.24	0.94 ± 0.36	1.00 ± 0.18	0.67 ± 0.04	1.00 ± 0.11‡	1.30 ± 0.25
	C57BL	1.00 ± 0.22	0.42 ± 0.08*	0.53 ± 0.12*	0.50 ± 0.07*	1.00 ± 0.16	0.59 ± 0.06*	0.75 ± 0.08*†	0.84 ± 0.09 †
<i>Cat</i>	ICR	1.00 ± 0.32	0.48 ± 0.23*	0.37 ± 0.13*	0.52 ± 0.23*	1.00 ± 0.76	0.66 ± 0.07	0.61 ± 0.07	0.76 ± 0.08
	C57BL	1.00 ± 0.11	0.29 ± 0.09*	0.31 ± 0.07*	0.33 ± 0.06*	1.00 ± 0.18	0.34 ± 0.07*	0.45 ± 0.07*	0.51 ± 0.09*†
<i>Gsr</i>	ICR	1.00 ± 0.20	0.84 ± 0.26	0.85 ± 0.24	0.73 ± 0.12	1.00 ± 0.34	0.84 ± 0.30	1.04 ± 0.36	1.11 ± 0.09
	C57BL	1.00 ± 0.21	0.48 ± 0.12*	0.82 ± 0.19†	0.82 ± 0.08†	1.00 ± 0.16	0.79 ± 0.05	1.28 ± 0.17	1.02 ± 0.22
<i>Gpx1</i>	ICR	1.00 ± 0.15	0.46 ± 0.11*	0.51 ± 0.13*	0.58 ± 0.15*	1.00 ± 0.13	0.71 ± 0.07	0.80 ± 0.24	0.95 ± 0.11
	C57BL	1.00 ± 0.12	0.42 ± 0.12*	0.58 ± 0.18*	0.56 ± 0.10*	1.00 ± 0.24	0.64 ± 0.07*	0.73 ± 0.17	0.87 ± 0.10 †
Fbrosis-related factors									
<i>Nox2</i>	ICR	1.00 ± 0.33	0.97 ± 0.32	1.21 ± 0.12	1.34 ± 0.37	1.00 ± 0.51	1.24 ± 0.67	1.19 ± 0.40	1.12 ± 0.64
	C57BL	1.00 ± 0.30	1.17 ± 0.30	1.35 ± 0.33	1.27 ± 0.23	1.00 ± 0.03	2.05 ± 0.42	1.36 ± 0.27	1.01 ± 0.48
<i>Tgfb</i>	ICR	1.00 ± 0.79	0.93 ± 0.67	0.89 ± 0.38	0.60 ± 0.28	1.00 ± 0.31	1.50 ± 0.62	1.36 ± 0.60	1.14 ± 0.51
	C57BL	1.00 ± 0.08	0.74 ± 0.09*	0.59 ± 0.07*†	0.69 ± 0.12*	1.00 ± 0.03	1.86 ± 0.40‡	1.41 ± 0.05‡	1.39 ± 0.34
<i>CollagenIa1</i>	ICR	1.00 ± 0.84	0.61 ± 0.09	0.44 ± 0.31	0.77 ± 0.49	1.00 ± 0.78	1.42 ± 0.76	1.42 ± 0.71	0.66 ± 0.24
	C57BL	1.00 ± 0.78	1.41 ± 0.77	1.41 ± 0.71	0.67 ± 0.24	1.00 ± 0.41	2.29 ± 0.29*	1.11 ± 0.83†	0.99 ± 0.35†

Data are represented as the mean ± SD. * $P < 0.05$ compared with each CD group (Dunnett's test). † $P < 0.05$ compared with each MCD group (Dunnett's test). ‡ $P < 0.05$ compared with each CD group (Steel-Dwass test). § $P < 0.05$ compared with each MCD group (Steel-Dwass test).

factor- κ B (NF- κ B) signal renders activation of hepatic stellate cells (HSCs) that more resistant to cell death, thereby promoting persistent HSC activation and fibrosis³⁸. Accordingly, an increased number of infiltrated macrophages may have contributed to the progression to fibrosis in C57BL/6J mice. Because the number of F4/80-positive macrophages in ICR mice also time-dependently increased in the present study, it is possible that a longer term of MCD administration in ICR mice might induce liver fibrosis. Therefore, these results also indicated that NASH in MCD-administrated C57BL/6J mice progresses earlier and is more severe than in ICR mice and suggested that C57BL/6J mice are a more suitable model for MCD-induced NASH than ICR mice.

Along with the strain difference, we also investigated the effect of BCP on the pathogenesis of NASH. BCP is a sesquiterpene that has many beneficial activities, including anti-inflammatory^{22, 23} and antioxidative stress²⁷. Histologically, hepatic steatosis and inflammation were attenuated by BCP coadministration at both 4 and 8 weeks in both strains, and liver fibrosis was attenuated at 8 weeks in C57BL/6J mice. The number of CD3- and F4/80-positive cells were also decreased by BCP coadministration. In addition, ALT was reduced to the control level by BCP coadministration. These results indicate that BCP exerts inhibitory effects against liver damage and inflammation in development and progression of NASH.

To elucidate the BCP-mediated inhibitory mechanism, the mRNA expression of inflammatory cytokines, oxidative stress-related factors and fibrosis-related factors was investigated. The mRNA expression of IL-6 was increased by MCD administration, and this increase was reduced by BCP coadministration at 8 weeks in ICR mice. On the other hand, the mRNA expression of IL-6 was not significantly different among the groups in C57BL/6J mice. A previous report revealed that IL-6-deficient mice showed attenuation of MCD-induced hepatic inflammation, but no influence on the degree of hepatic steatosis, compared with wild mice³⁹. From this finding, although the precise reason for the difference in IL-6 mRNA expression between the two strains was not unclear, it was suggested that BCP decreased the level of IL-6 mRNA but that this decrease may not be directly associate with inhibition of NASH development. As for MCP-1, its mRNA expression did not differ among the treatment groups at both 4 and 8 weeks in ICR mice, but it showed a tendency to increase in C57BL/6J mice as a result of MCD administration, and the increase was reduced by BCP coadministration at 8 weeks. The strain difference and BCP-induced amelioration relatively corresponded to the histological changes. MCP-1, also known as CCL2, is a potent chemoattractant for macrophages and is produced from various cells, especially HSCs⁴⁰. MCP-1 is also crucial for the development of hepatosteatosis, insulin resistance,

and obesity in mice fed a high-fat diet⁴¹. In addition, a previous study reported that blocking MCP-1 inhibited hepatic macrophage infiltration and steatohepatitis during chronic liver damage in a MCD model⁴². This finding may support our idea that decreased mRNA expression of MCP-1 partly contributes to the effect of BCP on attenuating NASH.

Hepatocytes with metabolic or toxic damage were responsible for induction of free radical chain reactions and lipid peroxidation, resulting in increased ROS formation, and increased ROS stimulated release of MCP-1 from HSCs in chronic liver injury⁴³. Also, oxidative stress is a central mechanism of hepatocellular injury in NASH⁴⁴. When the mRNA expression of antioxidant-related factors was investigated, the mRNA expressions of SOD2 and GPx1 were found to be decreased by MCD administration, and these decreases were returned to the control level by BCP coadministration in both strains. The mitochondrial capacity to control oxidative balance will collapse under continuous oxidative stress. Excess superoxide could be generated within injured mitochondria through electron leakage, and the resulting excess of superoxide would be converted to hydrogen peroxide by SOD2; conversion of hydrogen peroxide is carried out by the antioxidant enzyme GPx1. The combined approach of superoxide scavenging with replenishment of GSH, which is substrate for reduction of hydrogen peroxide, can be applied for treatment of NASH, as hydrogen peroxide, which is converted by SOD2, is also potent oxidant⁴⁵. A previous study reported that retinoic acid-related orphan receptor α (ROR α), which regulates diverse target genes associated with lipid metabolism, has a protective function against oxidative stress in the liver, and administration of JC1-40, a ligand of ROR α , decreased signs of liver injury, lipid peroxidation, and inflammation by inducing SOD2 and GPx1 expression in MCD-induced NASH mice⁴⁶. Thus, it was suggested that BCP-induced recovery of SOD2 and GPx1 mRNA expression attenuated steatohepatitis and decreased MCP-1 mRNA expression induced by MCD administration, resulting in amelioration of NASH progression.

The mRNA expression of Nox2 was increased by MCD administration at 8 weeks, and the increase was returned to the control level by BCP coadministration in C57BL/6J mice. Nox2, a membrane-bound enzyme complex, is involved in cellular respiratory bursts and free radical production in a variety of cells, including hepatocytes⁴⁷. Moreover, Nox2-generated oxidative stress is associated with severity of liver steatosis in patients with NAFLD⁴⁸. Some Nox isoforms, including Nox1, Nox2, and Nox4, are involved in the initiation of myofibroblasts activation and progression of liver fibrosis⁴⁹. Similar to the mRNA expression of Nox2, liver fibrosis was only observed in the present study in MCD-administrated C57BL/6J mice at 8 weeks, and it was attenuated by BCP coadministration (Fig. 2). Moreover, the mRNA expression of TGF- β and Collagen I α 1 showed similar changes (Table 5). Therefore, it was suggested that BCP decreases the mRNA expression of Nox2 and that it might partially contribute to preventing oxidative stress and fibrosis.

In conclusion, the obtained data suggested that, because the disease progressed relatively early, C57BL/6J mice were a more suitable model for MCD-induced NASH than ICR mice and that BCP has hepatoprotective effects against NASH, mainly through the inhibition of oxidative stress and following inflammation.

Disclosure of Potential Conflicts of Interest: The authors declare that they have no conflicts of interest.

References

1. Angulo P, and Lindor KD. Non-alcoholic fatty liver disease. *J Gastroenterol Hepatol.* **17**(Suppl): S186–S190. 2002. [[Medline](#)] [[CrossRef](#)]
2. Clark JM, Brancati FL, and Diehl AM. The prevalence and etiology of elevated aminotransferase levels in the United States. *Am J Gastroenterol.* **98**: 960–967. 2003. [[Medline](#)] [[CrossRef](#)]
3. Loomba R, and Sanyal AJ. The global NAFLD epidemic. *Nat Rev Gastroenterol Hepatol.* **10**: 686–690. 2013. [[Medline](#)] [[CrossRef](#)]
4. Miyashita T, Toyoda Y, Tsuneyama K, Fukami T, Nakajima M, and Yokoi T. Hepatoprotective effect of tamoxifen on steatosis and non-alcoholic steatohepatitis in mouse models. *J Toxicol Sci.* **37**: 931–942. 2012. [[Medline](#)] [[CrossRef](#)]
5. Kuczmarski RJ, Carroll MD, Flegal KM, and Troiano RP. Varying body mass index cutoff points to describe overweight prevalence among U.S. adults: NHANES III (1988 to 1994). *Obes Res.* **5**: 542–548. 1997. [[Medline](#)] [[CrossRef](#)]
6. Sanyal AJ, Campbell-Sargent C, Mirshahi F, Rizzo WB, Contos MJ, Sterling RK, Luketic VA, Shiffman ML, and Clore JN. Nonalcoholic steatohepatitis: association of insulin resistance and mitochondrial abnormalities. *Gastroenterology.* **120**: 1183–1192. 2001. [[Medline](#)] [[CrossRef](#)]
7. Chitturi S, Abeygunasekera S, Farrell GC, Holmes-Walker J, Hui JM, Fung C, Karim R, Lin R, Samarasinghe D, Liddle C, Weltman M, and George J. NASH and insulin resistance: Insulin hypersecretion and specific association with the insulin resistance syndrome. *Hepatology.* **35**: 373–379. 2002. [[Medline](#)] [[CrossRef](#)]
8. Marchesini G, and Forlani G. NASH: from liver diseases to metabolic disorders and back to clinical hepatology. *Hepatology.* **35**: 497–499. 2002. [[Medline](#)] [[CrossRef](#)]
9. Yang ZR, Wang HF, Zuo TC, Guan LL, and Dai N. Salidroside alleviates oxidative stress in the liver with non-alcoholic steatohepatitis in rats. *BMC Pharmacol Toxicol.* **17**: 16. 2016. [[Medline](#)] [[CrossRef](#)]
10. Caldwell SH, Oelsner DH, Iezzoni JC, Hespenheide EE, Battle EH, and Driscoll CJ. Cryptogenic cirrhosis: clinical characterization and risk factors for underlying disease. *Hepatology.* **29**: 664–669. 1999. [[Medline](#)] [[CrossRef](#)]
11. Green RM. NASH--hepatic metabolism and not simply the metabolic syndrome. *Hepatology.* **38**: 14–17. 2003. [[Medline](#)] [[CrossRef](#)]
12. Koteish A, and Diehl AM. Animal models of steatosis. *Semin Liver Dis.* **21**: 89–104. 2001. [[Medline](#)] [[CrossRef](#)]
13. London RM, and George J. Pathogenesis of NASH: animal models. *Clin Liver Dis.* **11**: 55–74, viii. 2007. [[Medline](#)]

- [CrossRef]
14. Machado MV, Michelotti GA, Xie G, Pereira TA, Boursier J, Bohnic B, Guy CD, and Diehl AM. Mouse models of diet-induced nonalcoholic steatohepatitis reproduce the heterogeneity of the human disease. *PLoS One*. **10**: e0127991. 2015. [Medline] [CrossRef]
 15. De Minicis S, and Brenner DA. Oxidative stress in alcoholic liver disease: role of NADPH oxidase complex. *J Gastroenterol Hepatol*. **23**(Suppl 1): S98–S103. 2008. [Medline] [CrossRef]
 16. Kono H, Rusyn I, Yin M, Gäbele E, Yamashina S, Dikalova A, Kadiiska MB, Connor HD, Mason RP, Segal BH, Bradford BU, Holland SM, and Thurman RG. NADPH oxidase-derived free radicals are key oxidants in alcohol-induced liver disease. *J Clin Invest*. **106**: 867–872. 2000. [Medline] [CrossRef]
 17. Koruk M, Taysi S, Savas MC, Yilmaz O, Akcay F, and Karakok M. Oxidative stress and enzymatic antioxidant status in patients with nonalcoholic steatohepatitis. *Ann Clin Lab Sci*. **34**: 57–62. 2004. [Medline]
 18. Chen Y, Yang Y, Miller ML, Shen D, Shertzer HG, Stringer KF, Wang B, Schneider SN, Nebert DW, and Dalton TP. Hepatocyte-specific Gclc deletion leads to rapid onset of steatosis with mitochondrial injury and liver failure. *Hepatology*. **45**: 1118–1128. 2007. [Medline] [CrossRef]
 19. Nan YM, Wu WJ, Fu N, Liang BL, Wang RQ, Li LX, Zhao SX, Zhao JM, and Yu J. Antioxidants vitamin E and 1-aminobenzotriazole prevent experimental non-alcoholic steatohepatitis in mice. *Scand J Gastroenterol*. **44**: 1121–1131. 2009. [Medline] [CrossRef]
 20. Wu ZR, Peng-Chen, Yang-Li, Li JY, Xin-Wang, Yong-Wang, Guo DD, Lei-Cui, Guan QG, and Li HY. Two cinnamoyloctopamine antioxidants from garlic skin attenuates oxidative stress and liver pathology in rats with non-alcoholic steatohepatitis. *Phytomedicine*. **22**: 178–182. 2015. [Medline] [CrossRef]
 21. Ni Y, Nagashimada M, Zhuge F, Zhan L, Nagata N, Tsutsui A, Nakanuma Y, Kaneko S, and Ota T. Astaxanthin prevents and reverses diet-induced insulin resistance and steatohepatitis in mice: A comparison with vitamin E. *Sci Rep*. **5**: 17192. 2015. [Medline] [CrossRef]
 22. Tambe Y, Tsujiuchi H, Honda G, Ikeshiro Y, and Tanaka S. Gastric cytoprotection of the non-steroidal anti-inflammatory sesquiterpene, beta-caryophyllene. *Planta Med*. **62**: 469–470. 1996. [Medline] [CrossRef]
 23. Lourens AC, Reddy D, Başer KH, Viljoen AM, and Van Vuuren SF. In vitro biological activity and essential oil composition of four indigenous South African *Helichrysum* species. *J Ethnopharmacol*. **95**: 253–258. 2004. [Medline] [CrossRef]
 24. Kubo I, Chaudhuri SK, Kubo Y, Sanchez Y, Ogura T, Saito T, Ishikawa H, and Haraguchi H. Cytotoxic and antioxidative sesquiterpenoids from *Heterotheca inuloides*. *Planta Med*. **62**: 427–430. 1996. [Medline] [CrossRef]
 25. Pichette A, Larouche PL, Lebrun M, and Legault J. Composition and antibacterial activity of *Abies balsamea* essential oil. *Phytother Res*. **20**: 371–373. 2006. [Medline] [CrossRef]
 26. Ghelardini C, Galeotti N, Di Cesare Mannelli L, Mazzanti G, and Bartolini A. Local anaesthetic activity of beta-caryophyllene. *Farmacologia*. **56**: 387–389. 2001. [Medline] [CrossRef]
 27. Singh G, Marimuthu P, de Heluani CS, and Catalan CA. Antioxidant and biocidal activities of *Carum nigrum* (seed) essential oil, oleoresin, and their selected components. *J Agric Food Chem*. **54**: 174–181. 2006. [Medline] [CrossRef]
 28. Calleja MA, Vieites JM, Montero-Meléndez T, Torres MI, Faus MJ, Gil A, and Suárez A. The antioxidant effect of β -caryophyllene protects rat liver from carbon tetrachloride-induced fibrosis by inhibiting hepatic stellate cell activation. *Br J Nutr*. **109**: 394–401. 2013. [Medline] [CrossRef]
 29. Cho JY, Chang HJ, Lee SK, Kim HJ, Hwang JK, and Chun HS. Amelioration of dextran sulfate sodium-induced colitis in mice by oral administration of beta-caryophyllene, a sesquiterpene. *Life Sci*. **80**: 932–939. 2007. [Medline] [CrossRef]
 30. Suzuki M, Adachi K, Ogawa Y, Karasawa Y, Katsuyama K, Sugimoto T, and Doi K. The Combination of Fixation Using PLP Fixative and Embedding in Paraffin by the AMeX Method is Useful for Immunohistochemical and Enzyme Histochemical Studies of the Lung. *N Tox Pathol*. **13**: 109–113. 2000. [CrossRef]
 31. Kleiner DE, Brunt EM, Van Natta M, Behling C, Contos MJ, Cummings OW, Ferrell LD, Liu YC, Torbenson MS, Unalp-Arida A, Yeh M, McCullough AJ, and Sanyal AJ; Nonalcoholic Steatohepatitis Clinical Research Network. Design and validation of a histological scoring system for nonalcoholic fatty liver disease. *Hepatology*. **41**: 1313–1321. 2005. [Medline] [CrossRef]
 32. Harrison SA, and Neuschwander-Tetri BA. Nonalcoholic fatty liver disease and nonalcoholic steatohepatitis. *Clin Liver Dis*. **8**: 861–879, ix. 2004. [Medline] [CrossRef]
 33. Kirsch R, Clarkson V, Shephard EG, Marais DA, Jaffer MA, Woodburne VE, Kirsch RE, and Hall PL. Rodent nutritional model of non-alcoholic steatohepatitis: species, strain and sex difference studies. *J Gastroenterol Hepatol*. **18**: 1272–1282. 2003. [Medline] [CrossRef]
 34. Weltman MD, Farrell GC, and Liddle C. Increased hepatocyte CYP2E1 expression in a rat nutritional model of hepatic steatosis with inflammation. *Gastroenterology*. **111**: 1645–1653. 1996. [Medline] [CrossRef]
 35. Mishra A, and Younossi ZM. Epidemiology and Natural History of Non-alcoholic Fatty Liver Disease. *J Clin Exp Hepatol*. **2**: 135–144. 2012. [Medline] [CrossRef]
 36. Fazel Y, Koenig AB, Sayiner M, Goodman ZD, and Younossi ZM. Epidemiology and natural history of non-alcoholic fatty liver disease. *Metabolism*. **65**: 1017–1025. 2016. [Medline] [CrossRef]
 37. Vizzutti F, Provenzano A, Galastri S, Milani S, Delogu W, Novo E, Caligiuri A, Zamara E, Arena U, Laffi G, Parola M, Pinzani M, and Marra F. Curcumin limits the fibrogenic evolution of experimental steatohepatitis. *Lab Invest*. **90**: 104–115. 2010. [Medline] [CrossRef]
 38. Pradere JP, Kluwe J, De Minicis S, Jiao JJ, Gwak GY, Dapito DH, Jang MK, Guenther ND, Mederacke I, Friedman R, Dragomir AC, Aloman C, and Schwabe RF. Hepatic macrophages but not dendritic cells contribute to liver fibrosis by promoting the survival of activated hepatic stellate cells in mice. *Hepatology*. **58**: 1461–1473. 2013. [Medline] [CrossRef]
 39. Mas E, Danjoux M, Garcia V, Carpentier S, Ségui B, and Levade T. IL-6 deficiency attenuates murine diet-induced

- non-alcoholic steatohepatitis. *PLoS One*. **4**: e7929. 2009. [[Medline](#)] [[CrossRef](#)]
40. Miura K, Yang L, van Rooijen N, Ohnishi H, and Seki E. Hepatic recruitment of macrophages promotes nonalcoholic steatohepatitis through CCR2. *Am J Physiol Gastrointest Liver Physiol*. **302**: G1310–G1321. 2012. [[Medline](#)] [[CrossRef](#)]
41. Kanda H, Tateya S, Tamori Y, Kotani K, Hiasa K, Kitazawa R, Kitazawa S, Miyachi H, Maeda S, Egashira K, and Kasuga M. MCP-1 contributes to macrophage infiltration into adipose tissue, insulin resistance, and hepatic steatosis in obesity. *J Clin Invest*. **116**: 1494–1505. 2006. [[Medline](#)] [[CrossRef](#)]
42. Baeck C, Wehr A, Karlmark KR, Heymann F, Vucur M, Gassler N, Huss S, Klussmann S, Eulberg D, Luedde T, Trautwein C, and Tacke F. Pharmacological inhibition of the chemokine CCL2 (MCP-1) diminishes liver macrophage infiltration and steatohepatitis in chronic hepatic injury. *Gut*. **61**: 416–426. 2012. [[Medline](#)] [[CrossRef](#)]
43. Zamara E, Galastri S, Aleffi S, Petrai I, Aragno M, Mastrocola R, Novo E, Bertolani C, Milani S, Vizzutti F, Vercelli A, Pinzani M, Laffi G, LaVilla G, Parola M, and Marra F. Prevention of severe toxic liver injury and oxidative stress in MCP-1-deficient mice. *J Hepatol*. **46**: 230–238. 2007. [[Medline](#)] [[CrossRef](#)]
44. Pessayre D. Role of mitochondria in non-alcoholic fatty liver disease. *J Gastroenterol Hepatol*. **22**(Suppl 1): S20–S27. 2007. [[Medline](#)] [[CrossRef](#)]
45. von Montfort C, Matias N, Fernandez A, Fucho R, Conde de la Rosa L, Martinez-Chantar ML, Mato JM, Machida K, Tsukamoto H, Murphy MP, Mansouri A, Kaplowitz N, Garcia-Ruiz C, and Fernandez-Checa JC. Mitochondrial GSH determines the toxic or therapeutic potential of superoxide scavenging in steatohepatitis. *J Hepatol*. **57**: 852–859. 2012. [[Medline](#)] [[CrossRef](#)]
46. Han YH, Kim HJ, Kim EJ, Kim KS, Hong S, Park HG, and Lee MO. ROR α decreases oxidative stress through the induction of SOD2 and GPx1 expression and thereby protects against nonalcoholic steatohepatitis in mice. *Antioxid Redox Signal*. **21**: 2083–2094. 2014. [[Medline](#)] [[CrossRef](#)]
47. Shah A, Kumar S, Simon SD, Singh DP, and Kumar A. HIV gp120- and methamphetamine-mediated oxidative stress induces astrocyte apoptosis via cytochrome P450 2E1. *Cell Death Dis*. **4**: e850. 2013. [[Medline](#)] [[CrossRef](#)]
48. Del Ben M, Polimeni L, Carnevale R, Bartimoccia S, Nocella C, Baratta F, Loffredo L, Pignatelli P, Violi F, and Angelico F. NOX2-generated oxidative stress is associated with severity of ultrasound liver steatosis in patients with non-alcoholic fatty liver disease. *BMC Gastroenterol*. **14**: 81. 2014. [[Medline](#)] [[CrossRef](#)]
49. Liang S, Kisseleva T, and Brenner DA. The Role of NADPH Oxidases (NOXs) in Liver Fibrosis and the Activation of Myofibroblasts. *Front Physiol*. **7**: 17. 2016. [[Medline](#)] [[CrossRef](#)]